

UCLA

UCLA Previously Published Works

Title

Diffusion MRI is superior to quantitative T2-FLAIR mismatch in predicting molecular subtypes of human non-enhancing gliomas

Permalink

<https://escholarship.org/uc/item/3h87r5nt>

Journal

Neuroradiology, 66(12)

ISSN

0028-3940

Authors

Cho, Nicholas S
Sanvito, Francesco
Le, Vièn Lam
et al.

Publication Date

2024-12-01

DOI

10.1007/s00234-024-03475-z

Peer reviewed



Diffusion MRI is superior to quantitative T2-FLAIR mismatch in predicting molecular subtypes of human non-enhancing gliomas

Nicholas S. Cho^{1,2,3,4} · Francesco Sanvito^{1,2} · Vièn Lam Le^{1,2,3} · Sonoko Oshima^{1,2} · Ashley Teraishi^{1,2} · Jingwen Yao^{1,2} · Donatello Telesca⁵ · Catalina Raymond^{1,2} · Whitney B. Pope¹ · Phioanh L. Nghiemphu^{6,7} · Albert Lai^{6,7} · Noriko Salamon¹ · Timothy F. Cloughesy^{6,7} · Benjamin M. Ellingson^{1,2,3,8,9}

Received: 30 May 2024 / Accepted: 30 September 2024 / Published online: 8 October 2024
© The Author(s) 2024

Abstract

Purpose This study compared the classification performance of normalized apparent diffusion coefficient (nADC) with percentage T2-FLAIR mismatch-volume (%T2FM-volume) for differentiating between IDH-mutant astrocytoma (IDHm-A) and other glioma molecular subtypes.

Methods A total of 105 non-enhancing gliomas were studied. T2-FLAIR digital subtraction maps were used to identify T2FM and T2-FLAIR non-mismatch (T2FNM) subregions within tumor volumes of interest (VOIs). Median nADC from the whole tumor, T2FM, and T2FNM subregions and %T2FM-volume were obtained. IDHm-A classification analyses using receiver-operating characteristic curves and multiple logistic regression were performed in addition to exploratory survival analyses.

Results T2FM subregions had significantly higher nADC than T2FNM subregions within IDHm-A with $\geq 25\%$ T2FM-volume ($P < 0.0001$). IDHm-A with $\geq 25\%$ T2FM-volume demonstrated significantly higher whole tumor nADC compared to IDHm-A with $< 25\%$ T2FM-volume ($P < 0.0001$), and both IDHm-A subgroups demonstrated significantly higher nADC compared to IDH-mutant oligodendroglioma and IDH-wild-type gliomas ($P < 0.05$). For classification of IDHm-A vs. other gliomas, the area under curve (AUC) of nADC was significantly greater compared to the AUC of %T2FM-volume ($P = 0.01$, nADC AUC = 0.848, %T2FM-volume AUC = 0.714) along with greater sensitivity. In exploratory survival analyses within IDHm-A, %T2FM-volume was not associated with overall survival ($P = 0.2$), but there were non-significant trends for nADC ($P = 0.07$) and tumor volume ($P = 0.051$).

Conclusion T2-FLAIR subtraction maps are useful for characterizing IDHm-A imaging characteristics. nADC outperforms %T2FM-volume for classifying IDHm-A amongst non-enhancing gliomas with preserved high specificity and increased sensitivity, which may be related to inherent diffusivity differences regardless of T2FM. In line with previous findings on visual T2FM-sign, quantitative %T2FM-volume may not be prognostic.

Keywords T2-FLAIR mismatch sign · IDH-mutant glioma · MRI · Diffusion MRI · Digital subtraction

Abbreviations

ADC	Apparent diffusion coefficient	MRI	glioma
AUC	Area under curve	nADC	Magnetic resonance imaging
IDH	Isocitrate dehydrogenase	NAWM	Normalized apparent diffusion coefficient
IDHm-A	Isocitrate dehydrogenase mutant astrocytoma	ROC	Normal appearing white matter
IDHm-O	Isocitrate dehydrogenase mutant oligodendroglioma	T2FM	Receiver-operating characteristic
IDHwt	Isocitrate dehydrogenase wild-type	T2FNM	T2-FLAIR mismatch
		%T2FM-Volume	T2-FLAIR non-mismatch
			Percentage T2-FLAIR mismatch

TCIA	volume
	The Cancer Imaging Archive
VOI	Volume of interest

Introduction

The “T2-FLAIR mismatch sign” (T2FM-sign) on T2-weighted MRI and T2-weighted FLAIR MRI is an established qualitative imaging feature with near 100% specificity for classifying isocitrate dehydrogenase-mutant 1p/19q-intact astrocytomas (IDHm-A) from IDH-mutant 1p/19q-codeleted oligodendrogliomas (IDHm-O) and IDH-wild-type (IDHwt) gliomas [1–9]. Non-invasive identification of IDHm-A—and perhaps more importantly, ruling out presence of aggressive IDHwt gliomas—can be beneficial in the up-front, treatment-naïve setting to guide treatment planning discussions in the relatively younger patient populations affected by IDHm-A compared to IDHwt gliomas [10], particularly with the recent advent of mutant IDH inhibitor targeted therapies [11].

Patel et al. first defined the T2FM-sign in IDHm-A as “presence or absence of complete/near-complete hyperintense signal on T2WI, and relatively hypointense signal on FLAIR except for a hyperintense peripheral rim” [1]. However, a limitation of the T2FM-sign has remained its low *sensitivity* for identifying IDHm-A. The seminal paper by Patel et al. observed sensitivities of 22.0 and 45.5% in two cohorts and a specificity of 100% in both cohorts [1], and low sensitivities have consistently been reported in subsequent studies [2, 7, 9]. There have been several approaches to potentially increase the sensitivity of the T2FM-sign. One approach has been to utilize looser definitions of the T2FM-sign, such as a visually-estimated tumor $\geq 25\%$ T2FM-volume threshold proposed by Lasocki et al. [12] or assessing only for T2-weighted FLAIR hyperintense rim & hypointense core and not using the T2-weighted MRI scan proposed by Li et al. [13], which achieved 100% specificity for IDHm-A with 63% and 71.3% sensitivity in their cohorts, respectively. Another approach has been to combine the T2FM-sign with quantitative MRI measures that have been previously well-described to classify IDHm-A from other molecular subgroups, such as combining T2FM-sign with apparent diffusion coefficient (ADC) from diffusion MRI [14] or normalized relative cerebral blood volume (nrCBV) from dynamic susceptibility contrast perfusion MRI [14]. However, one factor to consider about these prior approaches is that they were confined to the field’s *qualitative*, binarized (yes/no) assessment of T2FM-sign.

Recently, a *quantitative*, continuous assessment of T2FM volumetry using voxel-wise digital subtraction maps of T2-weighted and T2-weighted FLAIR MRI was introduced

[9]. Cho et al. observed that quantitative $\geq 42\%$ T2FM-volume achieved 100% specificity and 23.1% sensitivity for IDHm-A while $\geq 25\%$ T2FM-volume still achieved high specificity of 95% with 41.5% sensitivity for IDHm-A [9], which quantitatively validated prior qualitative results by Lasocki et al. [12] who proposed a threshold of $\geq 25\%$ T2FM-volume on visual evaluation for classifying IDHm-A.

Thus, there remains a present need for comparing and incorporating quantitative tumor %T2FM-volume with other well-known, quantitative imaging biomarkers for IDHm-A. For example, ADC values from diffusion MRI are known to be higher in IDHm-A compared to IDHm-O and IDHwt [15, 16]. ADC values are inversely related to cellular density [17], and a prior study using *qualitatively*-defined T2FM and T2-FLAIR non-mismatch (T2FNM) subregions observed that the T2FM-core subregion has higher ADC values than the T2FNM-rim subregion [18]. Given this finding, there remains a contemporary need of re-assessing previously established ADC group differences between IDHm-A and other molecular subtypes in the context of “mismatched” and “non-mismatched” IDHm-A as well as exploring subregional differences in “mismatched” IDHm-A.

The purpose of the present study was to utilize T2-FLAIR subtraction and normalized ADC (nADC) maps to characterize IDHm-A and IDHm-A subregions and to compare the classification performance of %T2FM-volume and nADC for differentiating between IDHm-A and other molecular subtypes. We hypothesized that: (i) T2-FLAIR subtraction map-defined T2FM subregions would have higher nADC compared to T2FNM subregions in IDHm-A with $\geq 25\%$ T2FM-volume (“mismatched” according to Cho et al. [9] and Lasocki et al. [12]), (ii) IDHm-A with $\geq 25\%$ T2FM-volume (“mismatched”) would have higher nADC compared to IDHm-A with $< 25\%$ T2FM-volume (“non-mismatched”), and (iii) nADC would outperform %T2FM-volume in classifying IDHm-A from IDHm-O and IDHwt gliomas due to the inherently low sensitivity of T2FM-sign. In exploratory analyses, we also theorized that (iv) %T2FM-volume would not be associated with survival, as was demonstrated in prior studies using the visual T2FM-sign [1, 4, 8].

Materials and methods

Patient cohort

A total of 645 patients with biopsy-proven gliomas across The Cancer Imaging Archive University of California San Francisco (TCIA UCSF) [19] and our institution were initially screened. Patients with the following inclusion criteria were studied: (1) non-enhancing, adult-type diffuse glioma

as classified by the World Health Organization 2021 criteria [20] (excluded $n=531$), (2) supratentorial (excluded $n=2$), (3) treatment-naïve except for biopsy (excluded $n=7$), and (4) molecular status available (IDH status for all lesions and 1p/19q status if IDH-mutant; excluded $n=1$). As a result, a total of 104 patients with 105 lesions were included in the study. This patient cohort was assessed in a prior study [9]. IDH and 1p/19q molecular status were determined by targeted next-generation sequencing, polymerase chain reaction sequencing, or immunohistochemistry and fluorescence in situ hybridization, respectively [21, 22]. Patient clinical data are summarized in Table 1.

Image acquisition and pre-processing

All patients underwent T2-weighted, T2-weighted FLAIR, and diffusion MRI on 3T scanners. T2-weighted and T2-weighted FLAIR were obtained using previously described protocols [9, 19]. ADC maps were generated from diffusion MRI datasets acquired with b-values of 0 and 1000 s/mm² (see Supplementary Table 1 for diffusion MRI protocol information). The TCIA data [19] were already pre-processed and registered to the 3D T2-weighted FLAIR MRI (Advanced Normalization Tools) and skull-stripped using “brain_mask” (https://www.github.com/ecalabr/brain_mask/), and the institutional data were pre-processed using an analogous pipeline of registering to the 3D T1-post-contrast MRI (*tkregister2*; Freesurfer [23]) *flirt*: Functional Magnetic Resonance Imaging of the Brain Software Library [24]) and skull-stripped using “HD-BET” (<https://github.com/MIC-DKFZ/HD-BET>) [25]. Normalized ADC (nADC) maps were created by voxel-wise dividing ADC by the mean ADC value of 3 spherical VOIs in the normal appearing white matter (NAWM) of the contralateral centrum semiovale [26].

Table 1 Patient characteristics

Characteristic	Patient Cohort ($n=104$ patients with $n=105$ lesions)
Age: Mean (Range)	42 (22–79)
Sex: M/F	59/45
Diagnosis: n (%)	
IDHm Astrocytoma	65 (61.9%)
Grade 2	44
Grade 3	20
Grade 4	1
IDHm Oligodendroglioma	18 (17.1%)
Grade 2	17
Grade 3	1
IDHwt Glioma	22 (21.0%)

IDHm=isocitrate dehydrogenase mutant; IDHwt=isocitrate dehydrogenase wild-type

T2-FLAIR subtraction maps

Voxel-wise T2-FLAIR digital subtraction maps were generated for each patient as previously described [9]. In brief, an additional, refined co-registration of the skull-stripped T2-weighted and T2-weighted FLAIR MRI was performed using FLIRT. Then, images were z-score- and NAWM-normalized to the contralateral centrum semiovale so that the NAWM signal intensity would be ~ 0 . Lastly, the normalized T2-weighted and T2-weighted FLAIR MRI were voxel-wise subtracted to create T2-FLAIR subtraction maps. A consistent threshold of 0 on the T2-FLAIR subtraction maps was used for all analyses, where positive values corresponded to T2FM-subregions and negative values corresponded to T2FNM-subregions within the tumor.

Brain tumor imaging analysis

All initial tumor VOI segmentations for the institutional data were performed by a lab member with 2 years of experience in tumor segmentation analysis (N.S.C.). The institutional and provided TCIA tumor segmentations were further refined via a semi-automated thresholding method using Analysis of Functional NeuroImages (AFNI) software (<https://afni.nimh.nih.gov>) [27] for consistency. Macroscopic cysts and CSF were excluded from the tumor segmentations. Lastly, a radiologist with 11 years of experience in neuroimaging analysis (S.O.) inspected all final tumor VOI segmentations while being blinded to the clinical data. T2FM and T2FNM subregion VOIs were then created from the tumor VOIs using the T2-FLAIR subtraction maps, and T2FM and T2FNM volumes were calculated to quantify percentage T2FM-volume (%T2FM-volume). IDHm-A were stratified based on $\geq 25\%$ T2FM-volume (“mismatched” IDHm-A) or $< 25\%$ T2FM-volume (“non-mismatched” IDHm-A) using previously-defined thresholds [9, 12]. Median nADC values from the tumor, T2FM subregion, and T2FNM subregion were also obtained.

Statistical analysis

GraphPad Prism software was used for statistical analyses. Paired t-tests were performed to assess differences in nADC between T2FM and T2FNM subregions IDHm-A with $\geq 25\%$ T2FM-volume. Repeated-measures ANOVA tests with post-hoc Holm-Sidak corrections were performed to assess group differences in nADC between different molecular types. Unpaired t-tests were performed to assess differences in nADC across IDHm-A tumor grades. Paired ROC curve analyses of %T2FM-volume and nADC to classify IDHm-A from IDHm-O/IDHwt (in line with the diagnostic usage of visual T2FM-sign [1, 12]), IDHm-A from

IDHm-O, and IDHm-A from IDHwt were performed, and the DeLong test was performed to compare the paired area under curve (AUC) values of nADC versus %T2FM-volume for each classification pairing. Multiple logistic regression was performed to assess the classification performance of the combination of nADC and %T2FM-volume and the combination of nADC, %T2FM-volume, and age for classifying IDHm-A. Survival analysis was restricted to the TCIA cohort-only because all data from the institutional data were censored in terms of overall survival, and one patient with 2 lesions was excluded from survival analysis. Log-rank tests were performed assessing any relationships of nADC, %T2FM-volume, tumor volume, and molecular status as categorical variables with overall survival. Univariate and

multivariate Cox survival analysis were performed on the same variables to assess any relationships with overall survival as continuous measures while controlling for factors such as age, extent of resection, and grade. Significance was set at $\alpha=0.05$ for all analyses.

Results

Four representative cases are shown in Fig. 1. Figure 1A shows a 36-year-old male patient who was diagnosed with an IDHm-A exhibiting a high median nADC of 3.02 and 53.5% T2FM-volume (“mismatched” IDHm-A). Figure 1B shows a 36-year-old female patient who was diagnosed with an IDHm-A exhibiting a moderately high median nADC of 2.15 nADC with only 10.9% T2FM-volume (“non-mismatched” IDHm-A). Figure 1C shows a 27-year-old female patient who was diagnosed with an IDHm-O exhibiting a lower median nADC of 1.78 and 6.8% T2FM-volume. Figure 1D shows a 75-year-old female patient who was diagnosed with an IDHwt glioma exhibiting a low median nADC of 1.62 and < 1% T2FM-volume.

Within IDHm-A exhibiting $\geq 25\%$ T2FM-volume (“mismatched”), there was significantly higher nADC in T2FM-subregions compared to T2FNM subregions ($P<0.0001$, mean difference=0.58, Fig. 2A). When assessing all IDHm-A, IDHm-A with $\geq 25\%$ T2FM-volume (“mismatched”) had significantly higher whole tumor nADC compared to IDHm-A with < 25% T2FM-volume (“non-mismatched”) ($P<0.0001$, Fig. 2B). Across glioma molecular subtypes while considering IDHm-A with $\geq 25\%$ T2FM-volume and IDHm-A with < 25% T2FM-volume as separate entities, both IDHm-A subgroups demonstrated significantly higher nADC compared to IDHm-O ($P<0.0001$ for $\geq 25\%$ T2FM-volume IDHm-A, $P=0.03$ for < 25% T2FM-volume IDHm-A, Fig. 2B) and IDHwt ($P<0.0001$ for both $\geq 25\%$ and < 25% T2FM-volume IDHm-A, Fig. 2B). There was also a trend towards significance for increased nADC in IDHm-O compared to IDHwt after multiple comparisons p-value correction ($P=0.09$, Fig. 2B). The T2FNM-subregion of IDHm-A with $\geq 25\%$ T2FM-volume demonstrated no significant difference in nADC with the whole tumor nADC of IDHm-A with < 25% T2FM-volume ($P=0.39$, Fig. 2C). T2FNM-subregions of IDHm-A with $\geq 25\%$ T2FM-volume still demonstrated significantly higher nADC compared to IDHm-O ($P=0.0063$, Fig. 2C) and compared to IDHwt ($P<0.0001$, Fig. 2C). There were no significant differences in nADC between grade 2 and grade 3 IDHm-A, whether across all IDHm-A ($P=0.56$), only IDHm-A $\geq 25\%$ T2FM-volume ($P=0.38$), or only IDHm-A < 25% T2FM-volume ($P=0.22$).

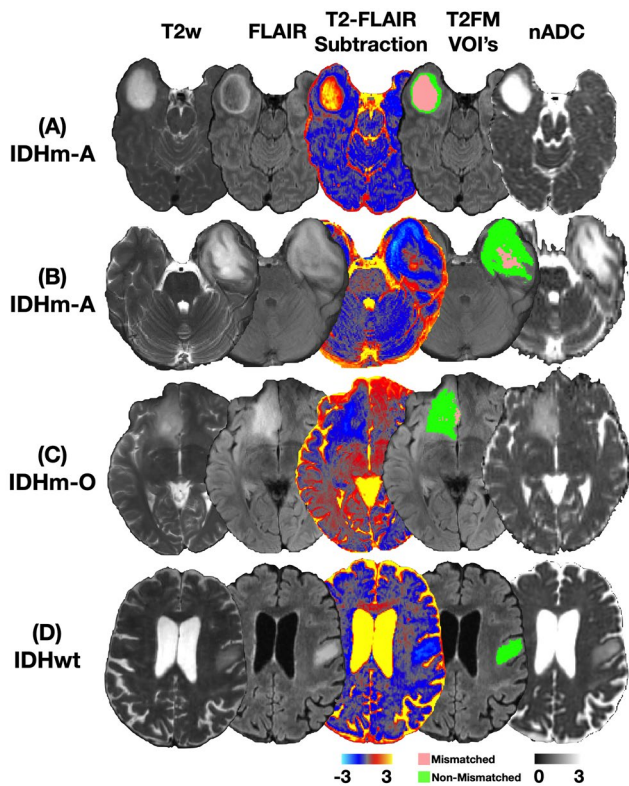


Fig. 1 Four representative cases with quantitative T2-FLAIR subtraction and nADC maps. **(A)** Patient A is a 36-year-old male diagnosed with IDH-mutant astrocytoma (IDHm-A) with 3.02 nADC and 53.5% T2-FLAIR mismatch volume (T2FM-volume) (“mismatched”). **(B)** Patient B is a 36-year-old female diagnosed with IDHm-A with 2.15 nADC and 10.9% T2FM-volume (“non-mismatched”). **(C)** Patient C is a 27-year-old female diagnosed with IDH-mutant oligodendroglioma (IDHm-O) with 1.78 nADC and 6.8% T2FM-volume. **(D)** Patient D is a 75-year-old female diagnosed with IDH-wild type (IDHwt) glioma with 1.62 nADC and < 1% T2FM-volume. Tumor segmentation volumes of interests (VOIs) denoting T2FM subregions (pink) and T2-FLAIR non-mismatch (T2FNM) subregions (green) are shown. IDHm-A=isocitrate dehydrogenase mutant astrocytoma; IDHm-O=isocitrate dehydrogenase mutant oligodendroglioma; IDHwt=isocitrate dehydrogenase wild type glioma; T2FM=T2-FLAIR mismatch; nADC=normalized apparent diffusion coefficient

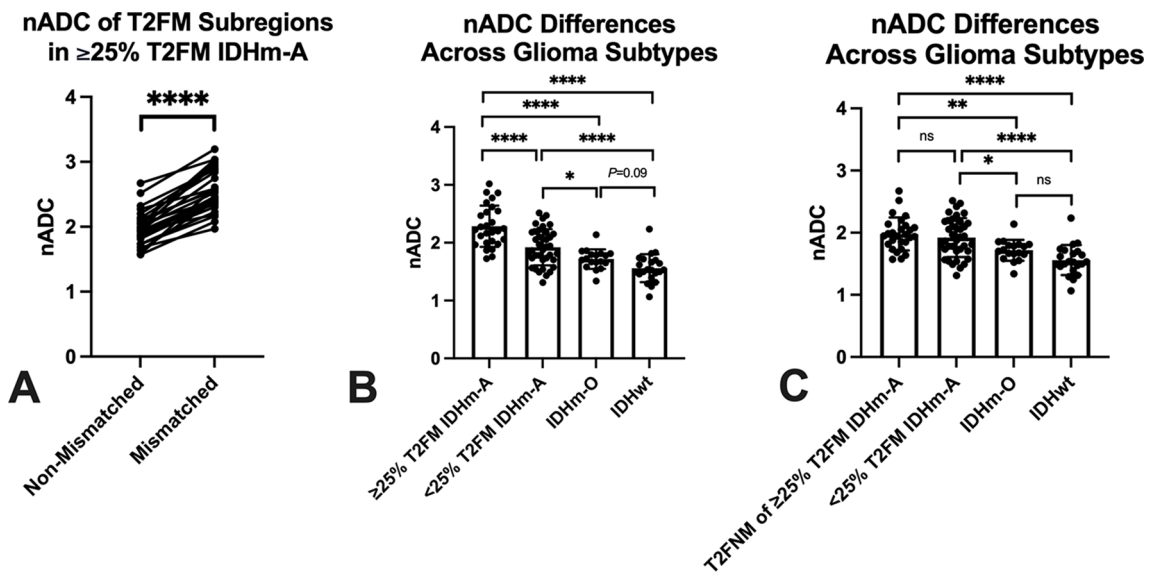


Fig. 2 Intra-tumoral and group nADC differences based on quantitative T2-FLAIR mismatch and glioma molecular subtypes. T2-FLAIR mismatch (T2FM) subregions of IDH-mutant astrocytomas (IDHm-A) with $\geq 25\%$ T2FM-volume had significantly higher nADC compared to T2-FLAIR non-mismatch (T2FNM) subregions ($P < 0.0001$, **A**). IDHm-A with $\geq 25\%$ T2FM-volume had significantly higher nADC compared to IDHm-A with $< 25\%$ T2FM-volume ($P < 0.0001$, **B**) and both IDHm-A subgroups had significantly higher nADC compared to IDH-mutant oligodendroglioma (IDHm-O) ($\geq 25\%$ T2FM-volume IDHm-A: $P < 0.0001$, $< 25\%$ T2FM-volume IDHm-A: $P = 0.03$, **B**)

and IDH-wild type glioma (IDHwt) (both $P < 0.0001$, **B**). T2FNM subregions of IDHm-A with $\geq 25\%$ T2FM-volume also had significantly higher nADC compared to IDHm-O ($P = 0.0063$, **C**) and IDHwt ($P < 0.0001$, **C**), but no difference with IDHm-A with $< 25\%$ T2FM-volume ($P = 0.39$, **C**) IDHm-A = isocitrate dehydrogenase mutant astrocytoma; IDHm-O = isocitrate dehydrogenase mutant oligodendroglioma; IDHwt = isocitrate dehydrogenase wild type glioma; T2FM = T2-FLAIR mismatch; nADC = normalized apparent diffusion coefficient; ns = not significant; * denotes $P < 0.05$; ** denotes $P < 0.01$; *** denotes $P < 0.001$; **** denotes $P < 0.0001$

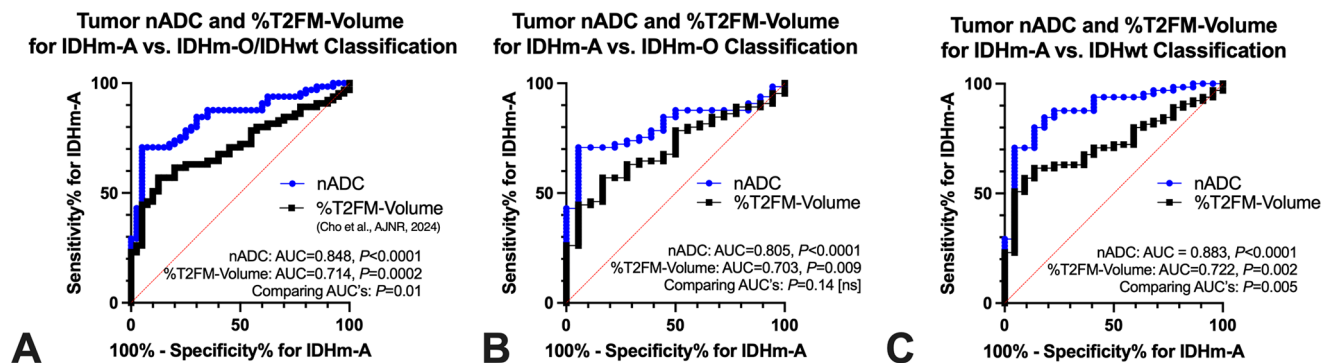


Fig. 3 Comparing diagnostic performance of tumor nADC and percentage T2-FLAIR mismatch volume for IDH-mutant astrocytoma classification. The area under curve (AUC) of nADC was significantly higher than the AUC of percentage T2-FLAIR mismatch volume (%T2FM-volume) for classifying IDH-mutant astrocytoma (IDHm-A) from IDH-mutant oligodendroglioma (IDHm-O) and IDH-wild type (IDHwt) ($P = 0.01$ comparing AUC's, **A**). The AUC of nADC was higher, but not significantly, than the AUC of %T2FM-volume

for classifying IDHm-A from IDHm-O ($P = 0.14$ comparing AUC's, **B**) and significantly higher for classifying IDHm-A from IDHwt ($P = 0.005$ comparing AUC's, **C**). Refer to Table 2 for summary cut-offs of %T2FM-volume and nADC for molecular classification IDHm-A = isocitrate dehydrogenase mutant astrocytoma; IDHm-O = isocitrate dehydrogenase mutant oligodendroglioma; IDHwt = isocitrate dehydrogenase wild type glioma; T2FM = T2-FLAIR mismatch; nADC = normalized apparent diffusion coefficient; ns = not significant

Paired ROC analyses were performed to compare the diagnostic performance of nADC vs. %T2FM-volume in differentiating IDHm-A from other molecular types. Both nADC and %T2FM-volume classified IDHm-A vs. IDHm-O/IDHwt individually ($P < 0.0001$ and $P = 0.0002$, respectively), but the AUC of nADC was significantly greater than the AUC of %T2FM-volume (nADC AUC = 0.848,

%T2FM-volume AUC = 0.714 [9], $P = 0.01$ comparing AUC's, Fig. 3A). In post-hoc analyses, the AUC of nADC remained greater than the AUC of %T2FM-volume for classifying IDHm-A just from IDHm-O (Fig. 3B) and IDHm-A just from IDHwt (Fig. 3C), although the AUC difference was significant only for classification from IDHwt (IDHm-A vs. IDHm-O: nADC AUC = 0.805,

%T2FM-volume AUC = 0.703, $P = 0.14$ comparing AUC's | *IDHm-A* vs. *IDHwt*: nADC AUC = 0.883, %T2FM-volume AUC = 0.722, $P = 0.005$ comparing AUC's). Table 2 summarizes empiric thresholds of nADC and %T2FM-volume for achieving 100% and ~95% specificity for the ROC analyses in Fig. 3, and the results show that nADC has greater sensitivity for *IDHm-A* compared to %T2FM-volume at these high-specificity thresholds (e.g. *IDHm-A* vs. *IDHm-O/IDHwt* with 95% specificity: nADC = 70.8% sensitivity, %T2FM-volume = 41.5% sensitivity). Multiple logistic regression results combining (i) nADC and %T2FM-volume and (ii) nADC, %T2FM-volume, and age demonstrated only *marginal* increases in AUC for classifying *IDHm-A* compared to using nADC-alone (*IDHm-A* vs. *IDHm-O/wt*: AUC 0.848 to 0.880, *IDHm-A* vs. *IDHm-O*: AUC 0.805 to 0.816, *IDHm-A* vs. *IDHwt*: AUC 0.883 to 0.938) (Supplementary Table 2).

For exploratory survival analysis, only 4 out of 44 patients with *IDHm-A* (9%) reached overall survival endpoint. Log-rank tests showed no significant association between %T2FM-volume and overall survival in *IDHm-A* ($P = 0.20$, $\geq 2\%$ T2FM-volume median survival = 2191 days, $< 2\%$ T2FM-volume median survival undefined, Mantel Haenszel hazard ratio = 4.76 (95% CI: 0.43–52.79),

Supplementary Fig. 1A), but there were trends towards significance for nADC ($P = 0.07$ with nADC ≥ 2.07 associated with longer OS, Mantel Haenszel hazard ratio = 0.12 (95% CI: 0.01–1.20), Supplementary Fig. 1B) and tumor volume ($P = 0.051$ with volume $\geq 60\text{mL}$ associated with shorter OS, Mantel Haenszel hazard ratio = 16.14 (95% CI: 0.98–264.9), Supplementary Fig. 1C) despite the large proportion of censored patients. Log-rank tests showed significant differences in overall survival between *IDHwt*, *IDHm-O*, and *IDHm-A* with $OS_{IDHwt} < OS_{IDHm-A} < OS_{IDHm-O}$ ($P < 0.0001$, Supplementary Fig. 1D). Cox survival analysis assessing overall survival in *IDHm-A* with %T2FM-volume, nADC, and tumor volume as continuous measures demonstrated no significant results in univariate analyses ($P > 0.05$) or multivariate analyses controlling for age, extent of resection, and grade ($P > 0.05$).

Discussion

Results from the current study suggest that diffusivity alterations may be a better discriminator for *IDHm-A* compared with the presence of T2FM. Our results suggest the previously-described low sensitivity of T2FM-sign for *IDHm-A* may not have necessarily been limited due to its previously qualitative and binarized assessment [1], but instead T2FM may be a feature with an inherently low-sensitivity for *IDHm-A* [9]. Consistent with the previous work from Lee et al. [14] who found that the combination of ADC characteristics and *visual* T2FM-sign improved the classification performance of *IDHm-A* from *IDHwt* gliomas, the present study observed increased performance when using the combination of nADC and *quantitative* %T2FM-volume; however, the present results also suggest that diffusion MRI alone may be sufficient to identify non-enhancing *IDHm-A* with preserved high specificity (~95–100%) and improved sensitivity compared to %T2FM-volume.

In corroboration of the findings reported by Foltyn et al. [18], the current study documented a significantly higher ADC in the T2-FLAIR subtraction map-defined T2FM-core subregions in *IDHm-A* compared to T2FNM-rim subregions. This finding may be explained by both the higher expression of mTOR-related genes in *IDHm-A* exhibiting T2FM [1, 28] resulting in higher proliferation [29, 30] and correspondingly lower ADC [31] in the rim as well as the presence of increased water mobility due to microcystic changes or enlarged intercellular space within the T2FM core region [1, 5, 8, 28]. Interestingly, the higher ADC in T2FM-areas raises a possibility that prior studies that established ADC differences across gliomas—namely, highest ADC in *IDHm-A*, then *IDHm-O*, then *IDHwt* [15, 16]—were potentially biased by the proportion of *IDHm-A* exhibiting

Table 2 Summary of nADC and %T2FM-Volume thresholds for classifying *IDH*-mutant astrocytomas with 100% specificity and ~95% specificity

Classification: <i>IDHm-A</i> vs. <i>IDHm-O/IDHwt</i>		
Threshold	Sensitivity (<i>IDHm-A</i>)	Specificity (<i>IDHm-A</i>)
nADC > 1.864	70.8%	95.0%
%T2FM-Volume > 25.00% ⁺	41.5%	95.0%
nADC > 2.240	29.2%	100%
%T2FM-Volume > 42.00% ⁺	23.1%	100%
Classification: <i>IDHm-A</i> vs. <i>IDHm-O</i>		
Threshold	Sensitivity (<i>IDHm-A</i>)	Specificity (<i>IDHm-A</i>)
nADC > 1.864	70.8%	94.4%
%T2FM-Volume > 22.05%	44.6%	94.4%
nADC > 2.145	43.1%	100%
%T2FM-Volume > 37.42%	26.2%	100%
Classification: <i>IDHm-A</i> vs. <i>IDHwt</i>		
Threshold	Sensitivity (<i>IDHm-A</i>)	Specificity (<i>IDHm-A</i>)
nADC > 1.849	70.8%	95.5%
%T2FM-Volume > 13.94%	50.8%	95.5%
nADC > 2.240	29.2%	100%
%T2FM-Volume > 41.77%	23.1%	100%

⁺ Previously reported in Cho et al., AJNR, 2024; *IDHm-A* = isocitrate dehydrogenase mutant astrocytoma; *IDHm-O* = isocitrate dehydrogenase mutant oligodendroglioma; *IDHwt* = isocitrate dehydrogenase wild type glioma; %T2FM-volume = percentage T2-FLAIR mismatch volume; nADC = normalized apparent diffusion coefficient

T2FM. As a result, the present study adds to the literature by re-assessing nADC glioma differences using $\geq 25\%$ T2FM-volume IDHm-A (“mismatched”) and $< 25\%$ T2FM-volume IDHm-A (“non-mismatched”) as separate tumor entities. Importantly, even IDHm-A with $< 25\%$ T2FM-volume still had higher nADC compared to IDHm-O and IDHwt, which suggests that there are diffusivity changes in IDHm-A inherent to their tumor biology that are not necessarily solely explained by the development of microcystic changes in T2FM-regions. Furthermore, these analyses demonstrate the value of T2-FLAIR subtraction maps in combination with whole tumor segmentations for characterizing “mismatched” IDHm-A and their tumor subregions via volumetric and quantitative image feature extraction.

Exploratory analysis found no significant association between quantitative %T2FM-volume within IDHm-A and survival, which appears in line with previous studies [1, 4, 8]. Similarly, lower nADC and larger tumor volume trended towards lower overall survival in IDHm-A, which is also consistent with prior studies [32–34]. However, it should be noted that our findings warrant cautious interpretation given that only 9% of the analyzed IDHm-A patients died during the observation period. While the median overall survival of the analyzed IDHm-A was still a considerable ~ 3 years including censored data, the median overall survival of low-grade IDHm-A is ~ 9 years [35], which presents a limitation of this study. Future studies with more mature survival data are necessary to confirm this observation.

Limitations

This study has limitations that should be addressed. Further analyses on expanded and/or independent external cohorts would be valuable to validate our findings that nADC is superior to quantitative %T2FM-volume for imaging-based classification of IDHm-A and that %T2FM-volume is not prognostic within IDHm-A. Additionally, a whole tumor segmentation-based processing pipeline was chosen for this study to maximize the technical rigor for quantifying %T2FM-volume and nADC. While suitable for research settings, this processing pipeline may not be as directly translatable to clinical settings. Future studies may consider utilizing single-slice or “hot-spot” nADC analyses as described in some prior studies on gliomas [16, 36]. Nevertheless, our proposed pipeline may have future clinical applicability for the management of non-enhancing gliomas as the automated capabilities of clinical PACS systems continue to expand, including with volumetric tumor segmentations and feature extraction [37, 38].

Conclusions

Diffusion MRI is better than %T2FM-volume for classifying IDHm-A amongst non-enhancing gliomas, and quantitative %T2FM-volume may not be prognostic in terms of predicting overall survival in non-enhancing human gliomas.

Supplementary Information The online version contains supplementary material available at <https://doi.org/10.1007/s00234-024-03475-z>.

Author contributions Study design: NSC, FS, BME. Data collection: NSC, FS, VLL, SO, AT, JY, CR, WBP, PLN, AL, TFC, NS, BME. Statistical analysis: NSC, FS, SO, DT, BME. Manuscript preparation: All authors.

Funding NIH NCI F30CA284809 (Cho), NIH NIGMS T32GM008042 (Cho), NIH NCI R01CA270027 (Ellingson, Cloughesy), NIH NCI R01CA279984 (Ellingson), DoD CDMRP CA220732 (Ellingson, Cloughesy), NIH NCI P50CA211015 (Ellingson, Cloughesy).

Declarations

Ethics approval The study was performed in line with the principles of the Declaration of Helsinki and in compliance with the Health Insurance Portability and Accountability Act.

Informed consent All patients in the institutional cohort provided informed consent.

Disclosures BME is on the advisory board and is a paid consultant for Medicenna, MedQIA, Servier Pharmaceuticals, Siemens, Janssen Pharmaceuticals, Imaging Endpoints, Kazia, Chimerix, Sumitomo Dainippon Pharma Oncology, ImmunoGenesis, Ellipses Pharma, Monteris, Neosoma, Alpheus Medical, Sagimet Biosciences, Sapience Therapeutics, Orbus Therapeutics, and the Global Coalition for Adaptive Research (GCAR).

TFC is cofounder, major stock holder, consultant and board member of Katmai Pharmaceuticals, holds stock for Erasca, member of the board and paid consultant for the 501c3 Global Coalition for Adaptive Research, holds stock in Chimerix and receives milestone payments and possible future royalties, member of the scientific advisory board for Break Through Cancer, member of the scientific advisory board for Cure Brain Cancer Foundation, has provided paid consulting services to Blue Rock, Vida Ventures, Lista Therapeutics, Stemline, Novartis, Roche, Sonalansense, Sagimet, Clinical Care Options, Ideology Health, Servier, Jubilant, Immvira, Gan & Lee, BrainStorm, Katmai, Sapience, Inovio, Vigeo Therapeutics, DNATrix, Tyme, SDP, Kintara, Bayer, Merck, Boehringer Ingelheim, VBL, Amgen, Kiyatec, Odonate Therapeutics QED, Medefield, Pascal Biosciences, Bayer, Tocagen, Karyopharm, GW Pharma, Abbvie, VBI, Deciphera, VBL, Agios, Genoece, Celgene, Puma, Lilly, BMS, Cortice, Novocure, Novogen, Boston Biomedical, Sunovion, Insys, Pfizer, Notable labs, Medqia, Trizel, Medscape and has contracts with UCLA for the Brain Tumor Program with Roche, VBI, Merck, Novartis, BMS, AstraZeneca, Servier. The Regents of the University of California (T.F.C. employer) has licensed intellectual property co-invented by TFC to Katmai Pharmaceuticals.

PLN has received grants/contracts from ERASCA, Millenium, Children’s Tumor Foundation, Dept of Defense, GCAR, Springsworks, and BMS and has received payment/honoraria from Alexion.

Conflict of interest The authors declare no conflicts of interest.


Open Access This article is licensed under a Creative Commons Attribution 4.0 International License, which permits use, sharing, adaptation, distribution and reproduction in any medium or format, as long as you give appropriate credit to the original author(s) and the source, provide a link to the Creative Commons licence, and indicate if changes were made. The images or other third party material in this article are included in the article's Creative Commons licence, unless indicated otherwise in a credit line to the material. If material is not included in the article's Creative Commons licence and your intended use is not permitted by statutory regulation or exceeds the permitted use, you will need to obtain permission directly from the copyright holder. To view a copy of this licence, visit <http://creativecommons.org/licenses/by/4.0/>.

References

- Patel SH, Poisson LM, Brat DJ, Zhou Y, Cooper L, Snuderl M, Thomas C, Franceschi AM, Griffith B, Flanders AE, Golfinos JG, Chi AS, Jain R (2017) T2–FLAIR mismatch, an imaging biomarker for IDH and 1p/19q status in Lower-grade gliomas: a TCGA/TCIA project. *Clin Cancer Res* 23:6078–6085. <https://doi.org/10.1158/1078-0432.CCR-17-0560>
- Broen MPG, Smits M, Wijnenga MMJ, Dubbink HJ, Anten M, Schijns O, Beckervordersandforth J, Postma AA, van den Bent MJ (2018) The T2-FLAIR mismatch sign as an imaging marker for non-enhancing IDH-mutant, 1p/19q-intact lower-grade glioma: a validation study. *Neuro Oncol* 20:1393–1399. <https://doi.org/10.1093/neuonc/noy048>
- Juratli TA, Tummala SS, Riedl A, Daubner D, Hennig S, Penson T, Zolal A, Thiede C, Schackert G, Krex D, Miller JJ, Cahill DP (2019) Radiographic assessment of contrast enhancement and T2/FLAIR mismatch sign in lower grade gliomas: correlation with molecular groups. *J Neurooncol* 141:327–335. <https://doi.org/10.1007/s11060-018-03034-6>
- Corell A, Ferreyra Vega S, Hoefling N, Carstam L, Smits A, Olsson Bontell T, Björkman-Burtscher IM, Carén H, Jakola AS (2020) The clinical significance of the T2-FLAIR mismatch sign in grade II and III gliomas: a population-based study. *BMC Cancer* 20:450. <https://doi.org/10.1186/s12885-020-06951-w>
- Deguchi S, Oishi T, Mitsuya K, Kakuda Y, Endo M, Sugino T, Hayashi N (2020) Clinicopathological analysis of T2-FLAIR mismatch sign in lower-grade gliomas. *Sci Rep* 10:10113. <https://doi.org/10.1038/s41598-020-67244-7>
- Jain R, Johnson DR, Patel SH, Castillo M, Smits M, van den Bent MJ, Chi AS, Cahill DP (2020) Real world use of a highly reliable imaging sign: T2-FLAIR mismatch for identification of IDH mutant astrocytomas. *Neurooncology* 22:936–943. <https://doi.org/10.1093/neuonc/noaa041>
- Kinoshita M, Arita H, Takahashi M, Uda T, Fukai J, Ishibashi K, Kijima N, Hirayama R, Sakai M, Arisawa A, Takahashi H, Nakanishi K, Kagawa N, Ichimura K, Kanemura Y, Narita Y, Kishima H (2021) Impact of Inversion Time for FLAIR Acquisition on the T2-FLAIR mismatch detectability for IDH-Mutant, Non-CODEL astrocytomas. *Front Oncol* 10. <https://doi.org/10.3389/fonc.2020.596448>
- van Garderen KA, Vallentgoed WR, Lavrova A, Niers JM, de Leng WWJ, Hoogstrate Y, de Heer I, Ylstra B, van Dijk E, Klein S, Draaisma K, Robe PAJT, Verhaak RGW, Westerman BA, French PJ, van den Bent MJ, Kouwenhoven MCM, Kros JM, Wesseling P, Smits M (2023) Longitudinal characteristics of T2-FLAIR mismatch in IDH-mutant astrocytomas: relation to grade, histopathology, and overall survival in the GLASS-NL cohort. *Neuro-Oncology Adv* 5:vdad149. <https://doi.org/10.1093/oaajnl/vdad149>
- Cho NS, Sanvito F, Le VL, Oshima S, Teraishi A, Yao J, Telesca D, Raymond C, Pope WB, Nghiemphu PL, Lai A, Cloughesy TF, Salamon N, Ellingson BM (2024) Quantification of T2-FLAIR mismatch in nonenhancing diffuse gliomas using Digital Subtraction. *AJNR Am J Neuroradiol* 45:188–197. <https://doi.org/10.3174/ajnr.A8094>
- Miller JJ, Gonzalez Castro LN, McBrayer S, Weller M, Cloughesy T, Portnow J, Andronesi O, Barnholtz-Sloan JS, Baumert BG, Berger MS, Bi WL, Bindra R, Cahill DP, Chang SM, Costello JF, Horbinski C, Huang RY, Jenkins RB, Ligon KL, Mellinghoff IK, Nabors LB, Platten M, Reardon DA, Shi DD, Schiff D, Wick W, Yan H, von Deimling A, van den Bent M, Kaelin WG, Wen PY (2023) Isocitrate dehydrogenase (IDH) mutant gliomas: a Society for Neuro-Oncology (SNO) consensus review on diagnosis, management, and future directions. *Neurooncology* 25:4–25. <https://doi.org/10.1093/neuonc/noac207>
- Mellinghoff IK, van den Bent MJ, Blumenthal DT, Touat M, Peters KB, Clarke J, Mendez J, Yust-Katz S, Welsh L, Mason WP, Ducray F, Umemura Y, Nabors B, Holdhoff M, Hottinger AF, Arakawa Y, Sepulveda JM, Wick W, Soffietti R, Perry JR, Giglio P, de la Fuente M, Maher EA, Schoenfeld S, Zhao D, Pandya SS, Steelman L, Hassan I, Wen PY, Cloughesy TF (2023) Vora-sidenib in IDH1- or IDH2-Mutant low-Grade Glioma. *N Engl J Med* 389:589–601. <https://doi.org/10.1056/NEJMoa2304194>
- Lasocki A, Buckland ME, Drummond KJ, Wei H, Xie J, Christie M, Neal A, Gaillard F (2022) Conventional MRI features can predict the molecular subtype of adult grade 2–3 intracranial diffuse gliomas. *Neuroradiology* 64:2295–2305. <https://doi.org/10.1007/s00234-022-02975-0>
- Li M, Ren X, Chen X, Wang J, Shen S, Jiang H, Yang C, Zhao X, Zhu Q, Cui Y, Lin S (2022) Combining hyperintense FLAIR rim and radiological features in identifying IDH mutant 1p/19q non-codeleted lower-grade glioma. *Eur Radiol* 32:3869–3879. <https://doi.org/10.1007/s00330-021-08500-w>
- Lee MK, Park JE, Jo Y, Park SY, Kim SJ, Kim HS (2020) Advanced imaging parameters improve the prediction of diffuse lower-grade gliomas subtype, IDH mutant with no 1p19q codeletion: added value to the T2/FLAIR mismatch sign. *Eur Radiol* 30:844–854. <https://doi.org/10.1007/s00330-019-06395-2>
- Leu K, Ott GA, Lai A, Nghiemphu PL, Pope WB, Yong WH, Liau LM, Cloughesy TF, Ellingson BM (2017) Perfusion and diffusion MRI signatures in histologic and genetic subtypes of WHO grade II–III diffuse gliomas. *J Neurooncol* 134:177–188. <https://doi.org/10.1007/s11060-017-2506-9>
- Thust SC, Hassanein S, Bisdas S, Rees JH, Hyare H, Maynard JA, Brandner S, Tur C, Jäger HR, Yousry TA, Mancini L (2018) Apparent diffusion coefficient for molecular subtyping of non-gadolinium-enhancing WHO grade II/III glioma: volumetric segmentation versus two-dimensional region of interest analysis. *Eur Radiol* 28:3779–3788. <https://doi.org/10.1007/s00330-018-5351-0>
- Ellingson BM, Malkin MG, Rand SD, Connelly JM, Quinsey C, LaViolette PS, Bedekar DP, Schmainda KM (2010) Validation of functional diffusion maps (fDMs) as a biomarker for human glioma cellularity. *J Magn Reson Imaging* 31:538–548. <https://doi.org/10.1002/jmri.22068>
- Foityn M, Nieto Taborda KN, Neuberger U, Brugnara G, Reinhardt A, Stichel D, Heiland S, Herold-Mende C, Unterberg A, Debus J, Deimling Av, Wick W, Bendszus M, Kickingereder P (2020) T2/FLAIR-mismatch sign for noninvasive detection of IDH-mutant 1p/19q non-codeleted gliomas: validity and pathophysiology. *Neuro-Oncology Adv* 2:vdaa004. <https://doi.org/10.1093/oaajnl/vdaa004>
- Calabrese E, Villanueva-Meyer JE, Rudie JD, Rauschecker AM, Baid U, Bakas S, Cha S, Mongan JT, Hess CP (2022) The University of California San Francisco Preoperative Diffuse

- Glioma MRI Dataset. *Radiol Artif Intell* 4:e220058. <https://doi.org/10.1148/ryai.220058>
20. Louis DN, Perry A, Wesseling P, Brat DJ, Cree IA, Figarella-Branger D, Hawkins C, Ng HK, Pfister SM, Reifenberger G, Soffietti R, von Deimling A, Ellison DW (2021) The 2021 WHO classification of tumors of the Central Nervous System: a summary. *Neuro Oncol* 23:1231–1251. <https://doi.org/10.1093/neuonc/noab106>
 21. Kline CN, Joseph NM, Grenert JP, van Ziffle J, Talevich E, Onodera C, Aboian M, Cha S, Raleigh DR, Braunstein S, Torkildson J, Samuel D, Bloomer M, Campomanes AGA, Banerjee A, Butowski N, Raffel C, Tihan T, Bollen AW, Phillips JJ, Korn WM, Yeh I, Bastian BC, Gupta N, Mueller S, Perry A, Nicolaides T, Solomon DA (2017) Targeted next-generation sequencing of pediatric neuro-oncology patients improves diagnosis, identifies pathogenic germline mutations, and directs targeted therapy. *Neurooncology* 19:699–709. <https://doi.org/10.1093/neuonc/now254>
 22. Lai A, Kharbanda S, Pope WB, Tran A, Solis OE, Peale F, Forrest WF, Pujara K, Carrillo JA, Pandita A, Ellingson BM, Bowers CW, Soriano RH, Schmidt NO, Mohan S, Yong WH, Seshagiri S, Modrusan Z, Jiang Z, Aldape KD, Mischel PS, Liau LM, Escovedo CJ, Chen W, Nghiemphu PL, James CD, Prados MD, Westphal M, Lamszus K, Cloughesy T, Phillips HS (2011) Evidence for sequenced molecular evolution of IDH1 mutant glioblastoma from a distinct cell of origin. *J Clin Oncol* 29:4482–4490. <https://doi.org/10.1200/jco.2010.33.8715>
 23. Fischl B (2012) FreeSurfer Neuroimage 62:774–781. <https://doi.org/10.1016/j.neuroimage.2012.01.021>
 24. Smith SM, Jenkinson M, Woolrich MW, Beckmann CF, Behrens TE, Johansen-Berg H, Bannister PR, De Luca M, Drobnjak I, Flitney DE, Niazy RK, Saunders J, Vickers J, Zhang Y, De Stefano N, Brady JM, Matthews PM (2004) Advances in functional and structural MR image analysis and implementation as FSL. *NeuroImage* 23(Suppl 1):S208–219. <https://doi.org/10.1016/j.neuroimage.2004.07.051>
 25. Isensee F, Schell M, Pflueger I, Brugnara G, Bonekamp D, Neuberger U, Wick A, Schlemmer HP, Heiland S, Wick W, Bendszus M, Maier-Hein KH, Kickingereder P (2019) Automated brain extraction of multisequence MRI using artificial neural networks. *Hum Brain Mapp* 40:4952–4964. <https://doi.org/10.1002/hbm.24750>
 26. Cho NS, Hagiwara A, Sanvito F, Ellingson BM (2023) A multi-reader comparison of normal-appearing white matter normalization techniques for perfusion and diffusion MRI in brain tumors. *Neuroradiology* 65:559–568. <https://doi.org/10.1007/s00234-022-03072-y>
 27. Cox RW (1996) AFNI: Software for Analysis and visualization of functional magnetic resonance neuroimages. *Comput Biomed Res* 29:162–173. <https://doi.org/10.1006/cbmr.1996.0014>
 28. Yamashita S, Takeshima H, Kadota Y, Azuma M, Fukushima T, Ogasawara N, Kawano T, Tamura M, Muta J, Saito K, Takeishi G, Mizuguchi A, Watanabe T, Ohta H, Yokogami K (2022) T2-fluid-attenuated inversion recovery mismatch sign in lower grade gliomas: correlation with pathological and molecular findings. *Brain Tumor Pathol* 39:88–98. <https://doi.org/10.1007/s10014-022-00433-6>
 29. Mecca C, Giambanco I, Donato R, Arcuri C (2018) Targeting mTOR in Glioblastoma: Rationale and Preclinical/Clinical evidence. *Dis Markers* 2018(9230479). <https://doi.org/10.1155/2018/9230479>
 30. Ryskalin L, Lazzeri G, Flaibani M, Biagioni F, Gambardella S, Frati A, Fornai F (2017) mTOR-Dependent Cell Proliferation in the Brain. *Biomed Res Int* 2017: 7082696. <https://doi.org/10.1155/2017/7082696>
 31. Karavaeva E, Harris RJ, Leu K, Shabihkhani M, Yong WH, Pope WB, Lai A, Nghiemphu PL, Liau LM, Chen W, Czernin J, Cloughesy TF, Ellingson BM (2015) Relationship between [18F]FDOPA PET uptake, apparent diffusion coefficient (ADC), and Proliferation Rate in recurrent malignant gliomas. *Mol Imaging Biol* 17:434–442. <https://doi.org/10.1007/s11307-014-0807-3>
 32. Feraco P, Bacci A, Ferrazza P, van den Hauwe L, Pertile R, Girlando S, Barbareschi M, Gagliardo C, Morganti AG, Petralia B (2020) Magnetic Resonance Imaging Derived Biomarkers of IDH Mutation Status and Overall Survival in Grade III Astrocytomas. *Diagnostics*
 33. Wu CC, Jain R, Radmanesh A, Poisson LM, Guo WY, Zagzag D, Snuderl M, Placantonakis DG, Golfinos J, Chi AS (2018) Predicting genotype and survival in Glioma using Standard Clinical MR Imaging Apparent Diffusion Coefficient images: a pilot study from the Cancer Genome Atlas. *Am J Neuroradiol* 39:1814. <https://doi.org/10.3174/ajnr.A5794>
 34. Carstam L, Corell A, Smits A, Dénes A, Barchéus H, Modin K, Sjögren H, Ferreyra Vega S, Bontell TO, Carén H, Jakola AS (2021) WHO Grade loses its prognostic value in molecularly defined diffuse Lower-Grade Gliomas. *Front Oncol* 11:803975. <https://doi.org/10.3389/fonc.2021.803975>
 35. Houillier C, Wang X, Kaloshi G, Mokhtari K, Guillemin R, Laffaire J, Paris S, Boisselier B, Idbaih A, Laigle-Donadey F, Hoang-Xuan K, Sanson M, Delattre JY (2010) IDH1 or IDH2 mutations predict longer survival and response to temozolomide in low-grade gliomas. *Neurology* 75:1560–1566. <https://doi.org/10.1212/WNL.0b013e3181f96282>
 36. Maynard J, Okuchi S, Wastling S, Busaidi AA, Almosawi O, Mbatha W, Brandner S, Jaunmuktane Z, Koc AM, Mancini L, Jäger R, Thust S (2020) World Health Organization Grade II/III Glioma Molecular Status: prediction by MRI morphologic features and apparent diffusion coefficient. *Radiology* 296:111–121. <https://doi.org/10.1148/radiol.2020191832>
 37. Aboian M, Bousabarah K, Kazarian E, Zeevi T, Holler W, Merkaç S, Cassinelli Petersen G, Bahar R, Subramanian H, Sunku P, Schrickel E, Bhawani J, Zawalich M, Mahajan A, Malhotra A, Payabvash S, Tocino I, Lin M, Westerhoff M (2022) Clinical implementation of artificial intelligence in neuroradiology with development of a novel workflow-efficient picture archiving and communication system-based automated brain tumor segmentation and radiomic feature extraction. *Front Neurosci* 16:860208. <https://doi.org/10.3389/fnins.2022.860208>
 38. Kaur M, Cassinelli Petersen G, Jekel L, von Reppert M, Varghese S, Dixe de Oliveira Santo I, Avesta A, Aneja S, Omuro A, Chiang V, Aboian M (2023) PACS-Integrated Tools for Peritumoral Edema Volumetrics provide additional information to RANO-BM-Based Assessment of Lung Cancer Brain metastases after Stereotactic Radiotherapy: a pilot study. *Cancers (Basel)* 15. <https://doi.org/10.3390/cancers15194822>

Authors and Affiliations

Nicholas S. Cho^{1,2,3,4}  · Francesco Sanvito^{1,2} · Vièn Lam Le^{1,2,3} · Sonoko Oshima^{1,2} · Ashley Teraishi^{1,2} · Jingwen Yao^{1,2} · Donatello Telesca⁵ · Catalina Raymond^{1,2} · Whitney B. Pope¹ · Phioanh L. Nghiemphu^{6,7} · Albert Lai^{6,7} · Noriko Salamon¹ · Timothy F. Cloughesy^{6,7} · Benjamin M. Ellingson^{1,2,3,8,9} 

✉ Benjamin M. Ellingson
bellingson@mednet.ucla.edu

¹ Department of Radiological Sciences, David Geffen School of Medicine, University of California, Los Angeles, Los Angeles, CA, USA

² UCLA Brain Tumor Imaging Laboratory (BTIL), Center for Computer Vision and Imaging Biomarkers, University of California, Los Angeles, Los Angeles, CA, USA

³ Department of Bioengineering, Henry Samueli School of Engineering and Applied Science, University of California, Los Angeles, Los Angeles, CA, USA

⁴ Medical Scientist Training Program, David Geffen School of Medicine, University of California, Los Angeles, Los Angeles, CA, USA

⁵ Department of Biostatistics, Fielding School of Public Health, University of California Los Angeles, Los Angeles, CA, USA

⁶ UCLA Neuro-Oncology Program, David Geffen School of Medicine, University of California, Los Angeles, Los Angeles, CA, USA

⁷ Department of Neurology, David Geffen School of Medicine, University of California, Los Angeles, Los Angeles, CA, USA

⁸ Department of Neurosurgery, David Geffen School of Medicine, University of California, Los Angeles, Los Angeles, CA, USA

⁹ Department of Psychiatry and Bibehavioral Sciences, David Geffen School of Medicine, University of California, Los Angeles, Los Angeles, CA, USA